

# Emulator-Based Optimization of a Semi-Active Hip Exoskeleton Concept: Sweeping Impedance Across Walking Speeds

Benjamin A. Shafer , *Graduate Student Member, IEEE*, Justine C. Powell, Aaron J. Young, *Member, IEEE*, and Gregory S. Sawicki, *Member, IEEE* 

Abstract—Objective: Semi-active exoskeletons combining lightweight, low powered actuators and passive-elastic elements are a promising approach to portable robotic assistance during locomotion. Here, we introduce a novel semi-active hip exoskeleton concept and evaluate human walking performance across a range of parameters using a tethered robotic testbed. Methods: We emulated semiactive hip exoskeleton (exo) assistance by applying a virtual torsional spring with a fixed rotational stiffness and an equilibrium angle established in terminal swing phase (i.e., via pre-tension into stance). We performed a 2-D sweep of spring stiffness x equilibrium position parameters (30 combinations) across walking speed (1.0, 1.3, and 1.6 m/s) and measured metabolic rate to identify device parameters for optimal metabolic benefit. Results: At each speed, optimal exoskeleton spring settings provided a ~10% metabolic benefit compared to zero-impedance (ZI). Higher walking speeds required higher exoskeleton stiffness and lower equilibrium angle for maximal metabolic benefit. Optimal parameters tuned to each individual (userdependent) provided significantly larger metabolic benefit than the average-best settings (user-independent) at all speeds except the fastest (p = 0.021, p = 0.001, and p = 0.098 at 1.0, 1.3, and 1.6 m/s, respectively). We found significant correlation between changes in user's muscle activity and changes in metabolic rate due to exoskeleton assistance, especially for muscles crossing the hip joint. Conclusion: A semi-active hip exoskeleton with spring-parameters personalized to each user could provide metabolic benefit across functional walking speeds. Minimizing muscle activity local to the exoskeleton is a promising approach for tuning assistance on-line on a user-dependent basis.

Manuscript received 19 November 2021; revised 2 April 2022 and 17 May 2022; accepted 10 June 2022. Date of publication 5 July 2022; date of current version 26 December 2022. This work was supported in part by the National Science Foundation (NSF) National Robotics Initiative (NRI) under Grant 1830215 to A.J.Y. and by the U.S. Army Natick Soldier Research, Development and Engineering Center (NSRDEC) under Grant W911QY18C0140 to G.S.S. (Corresponding author: Benjamin A. Shafer.)

Benjamin A. Shafer is with the George W. Woodruff School of Mechanical Engineering and the Institute for Robotics and Intelligent Machines, Georgia Institute of Technology, Atlanta, GA 30332 USA (e-mail: ben.shafer@gatech.edu).

Justine C. Powell, Aaron J. Young, and Gregory S. Sawicki are with the George W. Woodruff School of Mechanical Engineering and the Institute for Robotics and Intelligent Machines, Georgia Institute of Technology, USA.

This article has supplementary downloadable material available at https://doi.org/10.1109/TBME.2022.3188482, provided by the authors. Digital Object Identifier 10.1109/TBME.2022.3188482

Index Terms—Exoskeleton, Hip, Muscle Electromyography, Impedance Control, Metabolic Cost, Walking Speed.

#### I. INTRODUCTION

XOSKELETONS have been increasingly successful at providing enhanced walking performance by reducing the metabolic rate of the user [1]. Exoskeletons (exos) showing the largest metabolic benefits typically use control systems optimized to generate assistive torques at a target joint (e.g., ankle or hip) with timing and magnitude set specifically for a fixed gait (e.g., walk or run) and locomotor demand (e.g., speed or grade) on a treadmill [2]–[7]. These studies have provided a valuable foundation upon which the field is poised to expand. Indeed, a grand challenge remains to develop exos that can provide assistance outside the laboratory across the full functional range of locomotion modes (i.e., gaits, speeds, grades, stairs, unstructured terrain, etc.) used in everyday life. Toward this end, more research is needed to uncover strategies that are versatile enough to provide useful assistance across a broad range of locomotion behaviors in a form-factor that is streamlined and easy to use and maintain. Our goal here was to build on recent studies that have started to examine how exo assistance should change with gait [6], across speed [8], and according to the target joint for assistance [9]. Comprehensively examining users' physiological response to single-joint exo assistance strategies across walking speed is an important first step.

Taking clues from basic neuromechanics and energetics studies that address the joint-level mechanisms humans use to adapt locomotion behavior in response to changing demands could help guide versatile exoskeleton assistance strategies [10], [11]. For example, above self-selected walking speeds ( $>\sim 1.3$  m/s), there are stereotypical changes in lower-limb joint mechanics that accompany higher metabolic rate and metabolic cost of transport [10], [12]. As walking speed increases, both positive and negative mechanical work done on the center of mass increase in proportion to net metabolic rate [13]. To effectively handle the increased demand for mechanical work, humans increase muscle power output at all lower-limb joints, with hip (>40%) outpacing ankle (<40%) at the fastest speeds [10], [12], [14]. Observing which joints inject positive work into the gait cycle could provide guidance regarding where to place exo motors and when to activate them. Joint-level biomechanics

0018-9294 © 2022 IEEE. Personal use is permitted, but republication/redistribution requires IEEE permission. See https://www.ieee.org/publications/rights/index.html for more information.

can also be characterized by the relationship between the net muscle-tendon moment and the joint angle during steady-state movement, the quasi-stiffness. In fact, the quasi-stiffness of the lower-limb joints is modulated with speed. Throughout stance phase, quasi-stiffness increases with speed at all joints with the exception of the knee during weight acceptance [15]–[17]. The quasi-stiffness could provide guidance regarding stiffness and engagement timing of exo springs to provide unpowered elastic torque assistance. More studies are needed to understand whether and how exo assistance strategies should change in accordance with changing mechanical properties of the lower-limb joints across walking speed.

Given the goal to provide metabolic benefit across walking speeds, the hip joint emerges as a desirable target for exo assistance. Indeed, as previously mentioned, the hip muscletendons are major positive power generators during walking and become increasingly important at the fastest speeds [14]. It is also worth noting that the hip emerges as an even clearer power source uphill [11] and during accelerations [18], [19]. Further, simulation studies have predicted hip musculature may consume more energy during walking than muscles at the ankle [20]. This could be in part, due to morphological differences in ankle vs. hip muscle-tendons that make efficiency of positive work lower at the hip [21]. Focusing exo assistance on the least efficient lower-limb joint could yield more 'bang-for-buck' in terms of metabolic energy savings of the user. In addition to the physiological basis for focusing on the hip, it is also important to consider that the metabolic penalty due to added load of an exo placed at the hip would be small compared to other joints. Carrying added mass close to the body center or mass is relatively cheap compared to carrying it distally on the legs [22].

Despite the inability to generate positive mechanical power, passive devices have successfully enhanced walking performance at the hip, with modest metabolic benefits around 3% [23]–[25]. Success is mainly due to the lightweight nature of passive exos and tuning the elastic properties of the system (i.e., stiffness and equilibrium point) to generate useful assistance torque patterns that help the hip flex the leg into swing. A downside of the passive approach is that static mechanical properties of springs and dampers are static and may not be appropriate for all locomotion modes. To increase passive assistance adaptability, electromechanical clutches have been implemented in knee exoskeletons to modulate passive element properties and engagement but did not allow positive power generation. [26], [27]. Powered devices are bulky, require an energy source and may be harder to maintain, but can modulate torque assistance patterns on-line. In addition, powered exo assistance at the hip shows clear (and much larger) benefit, especially when timed to deliver torque during the early stance extension phase of walking [4], [28]–[30].

Hybrid designs that combine elements of both passive and active systems could allow adaptive torque assistance with lower actuator mass. For example, semi-active systems containing both motors and elastic elements could inject mechanical power in one gait phase and provide torque to support bodyweight in another, switching modes through a clutch-able transmission. Or perhaps low-power output motors could be used to merely

switch the mechanical properties of elastic elements rather than directly drive motion of the user. We contend that semi-active solutions could enable high performance of active systems with simplicity of passive systems.

A semi-active approach that combines passive and active elements has been applied to wearable devices, but mostly in prostheses. In one type of semi-active system, the passive components provide the assistance to the user while the active components are used to alter the mechanical properties or state of the passive components. Indeed, semi-active foot-ankle prostheses can modulate stiffness step by step to emulate physiological torques across modes like speeds, inclines, and stairs [31]–[34]. To our knowledge, semi-active lower-limb exo applications have not yet been realized, although there are creative actuator designs [35]–[38] and exciting theoretical concepts for how they might function [11], [39]. To explore these concepts, impedance control (torque based on virtual passive mechanical elements) can be implemented to mimic passive and semi-active devices to maximize performance, as seen with an ankle-foot prosthesis emulator [40]. Nevertheless, research addressing if/how the optimal passive properties (i.e., torque profile) of semi-active exo systems should change across modes and/or where active elements can best contribute is missing. Before spending time and effort building semi-active systems, lab-based emulator systems could be a useful tool to explore the utility and lay groundwork for semi-active exoskeletons.

Here, we employ a tethered exo emulator to apply hip torque to human users and examine whether the metabolic benefit of a virtual hip spring (i.e., a simple impedance) depends on its passive mechanical properties across walking speed. In short, we examined changes in users' metabolic rate across a wide range of stiffness and equilibrium angle of a virtual hip torsion spring [30 sets = 5 stiffness values (k) by 6 equilibrium angles] $(\theta_0)$  at each of three walking speeds (1.0, 1.3, and 1.6 m/s). We hypothesized that: (i) optimal 'semi-active' assistance would provide a metabolic benefit at each speed; but (ii) the optimal assistance parameters would mirror changes in physiological moment-angle behavior (i.e., quasi-stiffness [15]) with increasing speed. That is, with increasing walking speed we expected an increase in optimal hip exo spring stiffness (k) and a decrease in optimal hip exo spring equilibrium angle ( $\theta_0$ ) (i.e., biased closer to peak hip extension).

# II. METHODS

# A. Impedance Controller

To evaluate human locomotion performance with a semiactive hip exoskeleton (exo), we emulated the function of motorspring-clutch system using a tethered, cable-driven bilateral hip exoskeleton [41] (Human Motion Technologies, Pittsburgh, PA) while participants walked on an instrumented split-belt treadmill (Bertec, Inc.) (Fig. 1(a)) with assistive torque generated by a simple impedance controller (i.e., virtual torsional spring) (Fig. 1(b), top schematic). During assistance to the user (STATE 1, light gray), virtual Clutch 1 engaged the spring to the user and exo torques emulated a passive spring as a function of hip angle,  $\theta_{hip}$ , according to a preset passive spring stiffness, k, and equilibrium angle,  $\theta_0$  according to (1) below (Fig. 1(b), bottom

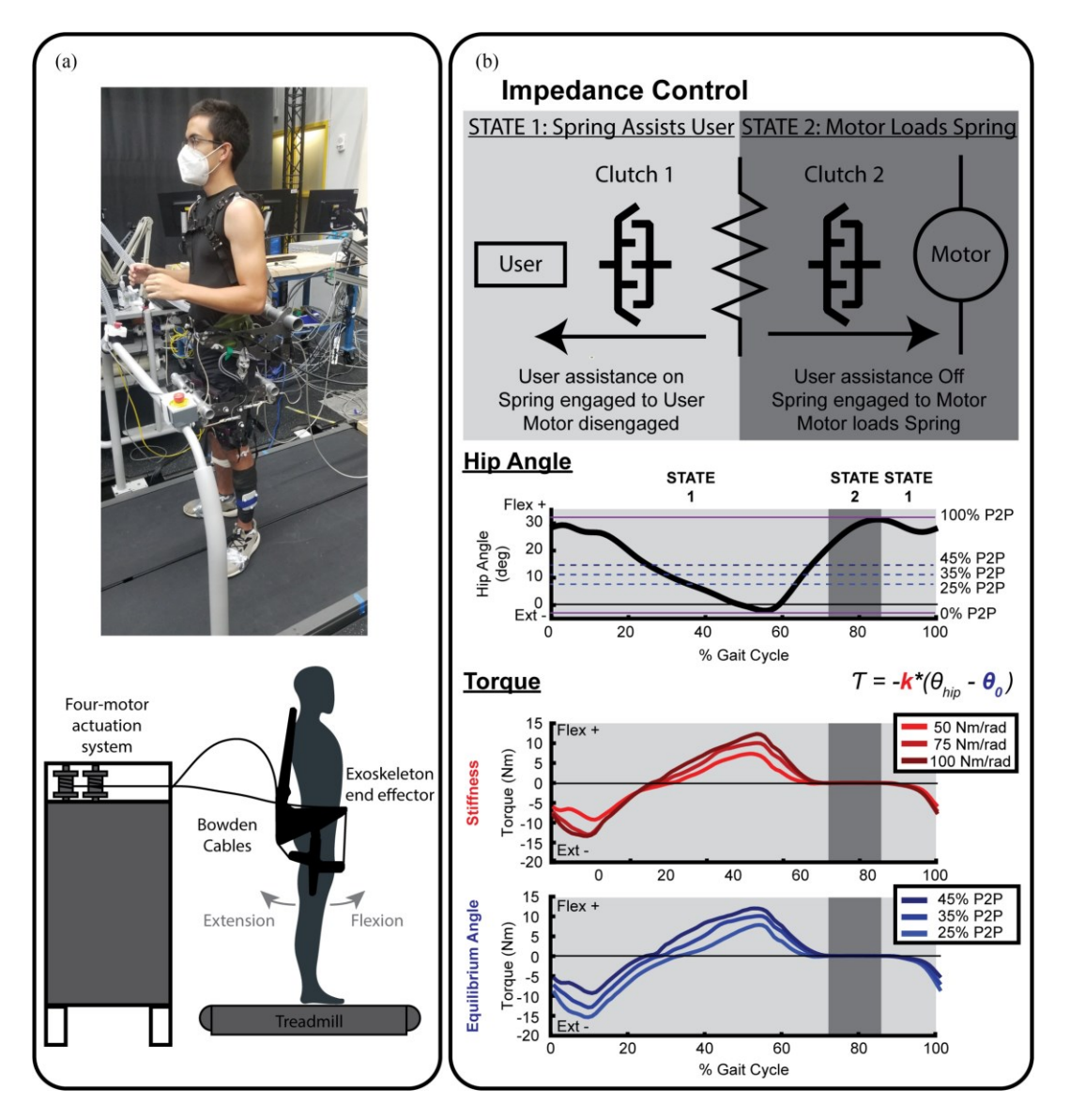


Fig. 1. Emulator-based evaluation of semi-active hip exoskeleton concept. (a) We used a tethered, cable-driven hip exoskeleton to apply both extension and flexion assistance torque for each leg. Four offboard motors pulled on Bowden cables to apply flexion and extension to each leg. (b) The applied torque profile was based on the concept of a semi-active device comprised of a motor, spring, and transmission with a two-state clutch mechanism. In State 1 (light gray), exoskeleton (exo) torque is transferred to the user according to a simple impedance (i.e., a virtual torsional spring) with a pre-set equilibrium angle ( $\theta_0$ ) and stiffness (k) (1). In this state, exo stiffness, k, modulated the magnitude of both flexion and extension torque assistance. Equilibrium angle,  $\theta_0$ , was calculated as a percentage of a 5-step average peak-to-peak (P2P) hip angle with peak extension = 0% and peak flexion = 100%.  $\theta_0$  modulated the timing of flexion torque onset/offset (smaller  $\theta_0$  = later flexion torque onset), as well as the relative magnitude of extension vs flexion torque (smaller  $\theta_0$  = larger extension torque bias at ground contact). In State 2 (dark gray), zero-impedance (ZI; no torque assisting or resisting the user) mode was engaged, starting when the hip angle flexed passed  $\theta_0$  ( $\sim$ 70% gait cycle) and ending with peak hip flexion. Simultaneously, a motor loading action was used to coil the virtual spring, developing extension torque internally, which was released by a clutch set to unlock at the onset of late swing hip extension ( $\sim$ 90% gait cycle).

timeseries graphs).

$$\tau = -\mathbf{k} \left( \theta_{hip} - \mathbf{\theta}_0 \right) \tag{1}$$

During STATE 1, torque assistance was applied independently to each leg for both hip flexion (pos.) and extension (neg.). As a key feature of the semi-active concept, we also implemented a zero-impedance (ZI) output period, a control strategy where no torque or resistance applied to the user (STATE 2 – dark gray in Fig. 1(b)). STATE 2 was implemented during swing phase starting when the hip angle reached  $\theta_0$  and ending when the hip

angle reversed direction at peak hip flexion (Fig. 1(b), bottom timeseries graphs). Without STATE 2, ZI output to the user, a fully passive device would resist user hip flexion, loading the spring while it applies extension torque, potentially impeding natural motion of the leg during swing [42]. Conceptually at the onset of STATE 2, the virtual Clutch 1 disengaged the spring from the user and Clutch 2 engaged the spring to the motor. this prevented extension torque transmission to the user via Clutch 1 and isolated motor-spring interaction through Clutch 2 The virtual motor then internally winded the exo spring (Fig. 1(b), top

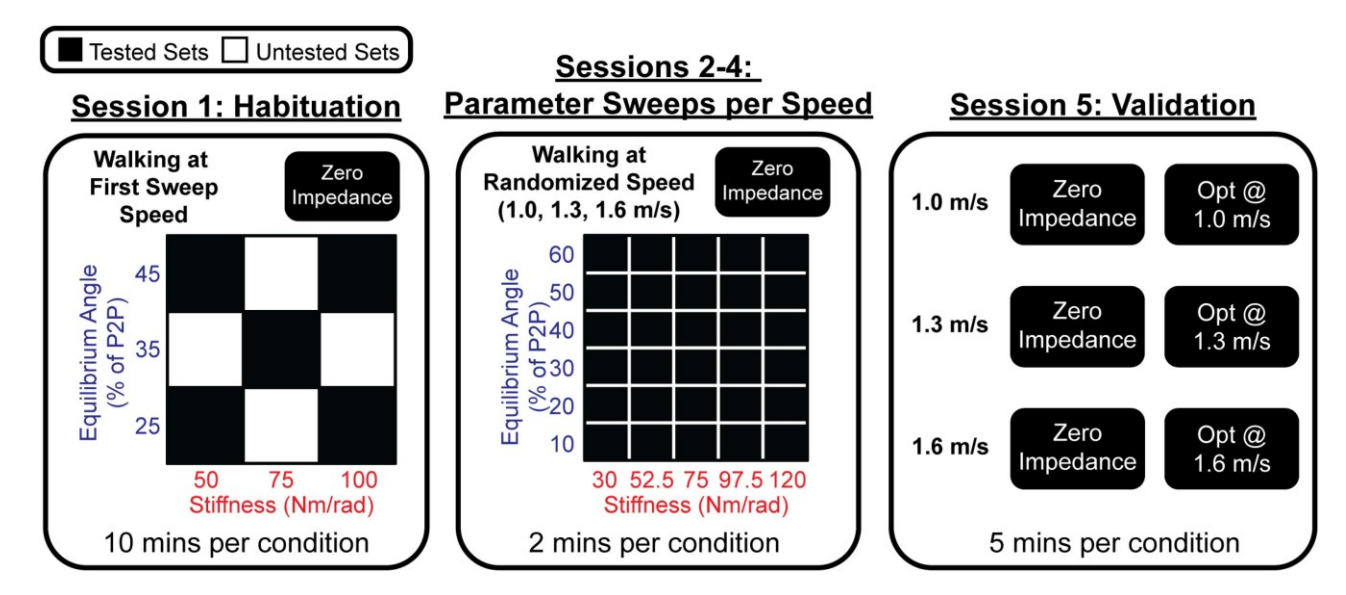


Fig. 2. Multi-session protocol to find optimal impedance parameters across speeds. The experimental protocol was split into 5 sessions. Session 1 (left) explored 5 spring parameter combinations and zero-impedance (ZI) for 10 minutes each, allowing the user to acclimate to walking with hip exo assistance at the first parameter sweep speed. Sessions 2–4 (middle) tested x30 parameter sets spanning the full range of k-  $\theta_0$  impedance control space while recording users' metabolic rate and electromyography. A metabolic cost to exo parameter surface was created for each walking speed and the parameter set that minimized metabolic cost was used as the optimal for that speed (user-dependent). During Session 5 (right), users walked at all three speeds with zero-impedance and the user-dependent optimal condition for that speed to validate results.

schematic). Finally, at the time of maximum hip flexion in late swing, coiled spring energy would be released to the user (State 2 -> State 1), by disengaging Clutch 2 and engaging Clutch 1, driving a pre-stance swing leg retraction to help propel the user via hip exo extension torque (Fig. 1(b), bottom timeseries graphs). A ramping function was implemented at extension torque onset to ensure high torques were not applied in a rapid manner, which was uncomfortable to some pilot participants. Exo stiffness (k) (Nm/rad) modulates the total torque range, increasing both flexion and extension peak torques with higher stiffnesses (Fig. 1(b), red). Exo equilibrium angle ( $\theta_0$ ) modulates the ratio between flexion and extension peak torques by shifting the torque along the vertical axis (Fig. 1(b), blue). To account for changes in range of motion with assistance, equilibrium angle was denoted as a percentage of a 5-step average peak-to-peak (P2P) range of motion, with peak flexion as 100% and peak extension as 0%. As equilibrium angle increased, the user experienced higher peak flexion torque, a lower peak extension torque, and flexion assistance starting earlier and ending later in the gait cycle.

We determined the ranges for stiffness and equilibrium angles based on pilot study data and peak torque. During pilot studies, we found parameter sets with higher than 60% equilibrium angle generated metabolic penalties compared to 60% and lower values. Having the range of equilibrium angles, we then tuned stiffness ranges to elicit peak torques from 5 Nm minimum to approximately 50 Nm maximum. The maximum limit was chosen based on [43] as their metabolically optimal hip only peak torque spline assistance was around 0.6–0.7 Nm/kg and the average weight of our pilot participants was around 70 kg. The inform increments between equilibrium angle and stiffness values were chosen to approximate 5 Nm, the minimum change

in torque seen to elicit metabolic cost differences around 4% or above.

# B. Study Protocol

We recruited 10 healthy young adults to participate in the study (7M/3F;  $67.76 \pm 10.62$  kg,  $172.2 \pm 9.4$  cm). This study protocol was approved by the Georgia Institute of Technology Institutional Review Board (Protocol #: H18067 starting on June 14th, 2018) and all participants supplied voluntary consent to participate. For each participant, we implemented a 5-session protocol with three distinct purposes: (1) habituate the user to the device and measurement equipment, (2) create a metabolic cost to exoskeleton parameter landscape for a sweep of many (k- $\theta_0$ ) combinations across a functional range of walking speeds (1.3–1.6 m/s), and (3) independently validate user metabolic performance with optimal exo settings across speeds (Fig. 2).

1) Habituation: Session 1 involved user habituation to the device, the controller, and metabolic measurement system (explained in next section). Habituation, at least 25–30 mins, is necessary for the user to acclimate to wearing the exo and to develop efficient walking patterns utilizing assistance [44], [45]. To accommodate for the variety of assistance profiles the user would experience during the sweep sessions, we extended the habituation session to 60 minutes. Walking speed was chosen as the first of the randomized walking speeds (to be used as the sweep order in Sessions 2-4). Users first walked at a zero-impedance (ZI) condition (no assistance/resistance applied for the entire gait cycle), then at 5 randomized exo spring parameter sets ([50, 25], [50, 45], [75, 35], [100, 25], & [100, 45] with [stiffness k, in Nm/rad, equilibrium angle  $\theta_0$  in % P2P range of motion]) for 10 minutes each (Fig. 2, left).

2) Exo Spring Parameter Sweeps Per Speed: To measure how metabolically optimal exo control parameters changed across walking speeds, we swept all combinations of 5 stiffness values (k = 30, 52.5, 75, 97.5, & 120 Nm/rad) and 6 equilibrium angles ( $\theta_0 = 10, 20, 30, 40, 50, \& 60\%$ ) at each of three walking speeds (1.0, 1.3, and 1.6 m/s) in randomized order (Fig. 2, middle). Each parameter set and initial ZI condition was applied for 2 minutes while we measured metabolic rate and lower-limb muscle electromyography (EMG). To determine the metabolically optimal exo spring parameter set for each speed, a metabolic cost - exo parameter landscape was created using a 2nd order fit across stiffness, k, and a 3rd order fit across equilibrium angle,  $\theta_0$ , a multidimensional application of [46]. Pilot testing revealed that this was the lowest order fit on each parameter that provided reasonably low error without overfitting. We then analytically solved for the k- $\theta_0$  parameter combination that minimized the metabolic rate in the landscape and used this optimal set for validation. We pilot tested real-time or "body/human-in-the-loop" protocols using online optimization algorithms for this study [47], [48] but did not choose them as they would not consistently sample cost across the entire parameter space or provide optimal parameters within a lower number of samples for this lower multidimensional problem. If there were 3 or more parameters, we believe an online optimization algorithm would provide a more rapid optimal solution than our proposed method.

We note, for most participants, the optimal  $(k-\theta_0)$  set was in between sweep values and thus was not experienced by the user before the validation session.

3) Validation: The final session (Session 5) was used to compare the metabolically optimal exo parameter set for each speed for each individual (user-dependent) to ZI at that speed (Fig. 2, right). Testing by speed was done in the same randomized order as the sweeps, completing all conditions at that speed then moving to the next. Each condition lasted 5 minutes while we measured metabolic rate and lower-limb muscle electromyography (EMG).

## C. Metabolic Cost

Metabolic cost was measured via indirect calorimetry. Breathby-breath oxygen consumption and carbon dioxide production were measured and used to calculate body mass specific gross metabolic rate (W/kg) using the Brockway Equation [49]. For the exo parameter sweep sessions (Session 2-4), steady-state metabolic rate was estimated as the asymptote of a first order fit to 2 minutes of data [50]. For the validation session (Session 5), steady-state was calculated as the average metabolic rate from the last minute of each 5-minute bout. We conducted a metabolic cost comparison between user-dependent and user-independent impedance parameters, which we detail in Section II-E. We note, due to an equipment malfunction, the zero-impedance (ZI) trial for one participant during the 1.6 m/s validation session was only 3.5 minutes long due, so the average of the last 30s of the trial was used for the steady state metabolic rate. Study wide, we computed the percentage difference in metabolic rate using the ZI condition from that same session as baseline.

# D. Electromyography

Muscle activity was measured via surface electromyography (EMG) for eight muscles: tibialis anterior (TA), medial gastrocnemius (MG), soleus (SOL), vastus medialis (VM), rectus femoris (RF), biceps femoris (BF), gluteus maximus (GMa), and gluteus medius (GMe). EMG sensors (Delsys, Inc.) were placed over each muscle on the left leg according to standard methods [51].

Raw EMG signals were processed through a bandpass Butterworth filter with cutoff frequencies of 20 and 400 Hz before being rectified. Each rectified signal was normalized by dividing by the peak magnitude of the corresponding signal (same speed, same muscle) from the zero-impedance (ZI) trial. Using ground reaction force (GRF) measurements, the EMG signals were then clipped to only include full strides in the analyses.

Next, each processed signal was integrated with respect to time; and the magnitude of the time-integral was divided by the total time of the processed signal to get the average normalized muscle activity for that trial. Then, to calculate the change in muscle activity due to each exo control parameter set, we subtracted the average muscle activity from the corresponding ZI trial in that session. For one participant walking in the 1.3 m/s condition, data from the ZI trial had an excessively low signal-to-noise ratio, so no analysis was done with the participant for that speed.

# E. User-Dependent vs. User- Independent Comparisons

Both user-dependent and user-independent approaches were used to report optimal exo parameter sets and the associated changes in metabolic cost across walking speeds (e.g., see Fig. 3). User-dependent measures (both optimal exo parameter sets  $(k-\theta_0)$  and the estimated change in metabolic cost ( $\Delta$  % from zero-impedance (ZI)) were defined using the global minimum of the fit to each individual user's metabolic cost landscape from the sweep grid points (Supp. Fig. 1) and then averaged across participants. This approach accounts for each individual user's unique relationship between exo assistance parameters and metabolic cost while decreasing biasing effects from noisy metabolic measurements and estimations. User-independent measures were defined using a single across-participant average metabolic cost landscape in exo parameter space  $(k-\theta_0)$ . Thus, the user-independent metabolic cost minimum ( $\Delta$  % from ZI) and the exo parameters that generated it  $(k-\theta_0)$  were single values without any variance. As such, the user-independent approach assumes a 'generic' average user, and effectively smooths differences between participants, keeping only the major trends across participants intact.

# F. Statistical Analyses

We set out to examine whether the metabolically optimal hip exo parameters could reduce gross metabolic rate compared to zero-impedance (ZI) at each walking speed (Hypothesis 1); and whether the optimal exo parameters were different for different speeds (Hypothesis 2). Hypothesis 1 was tested using three separate within-speed, one-factor repeated measures ANOVA

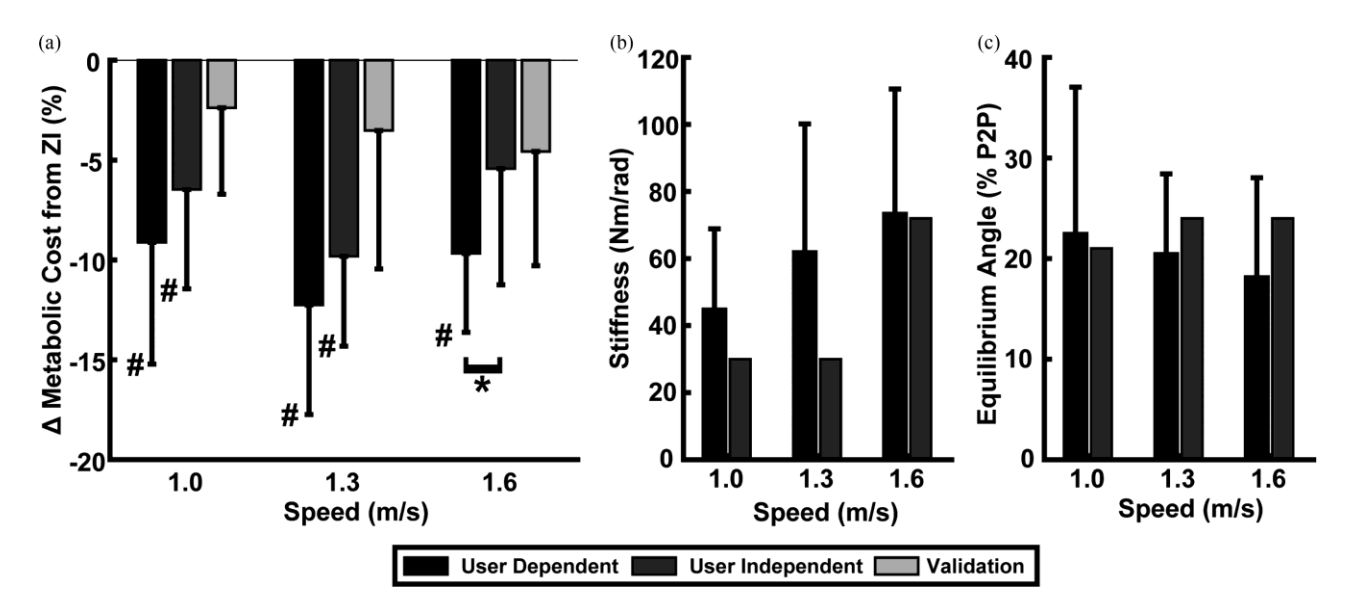


Fig. 3. Metabolic benefit and optimal hip exoskeleton impedance parameters  $(k-\theta_0)$  across walking speed. (a) Optimal metabolic benefit ( $\Delta\%$  change from zero-impedance (ZI)) for each walking speed. User-dependent values (black) are mean  $\pm$  SD taken from the fit to each individual participant's metabolic cost landscape (see Supp. Fig. 1). User-independent value (dark gray) is taken from the grid point that yielded the minimum  $\Delta$  metabolic rate from ZI for the metabolic cost surface fitted to the across-participant average data (hence no SD). Validation values (light gray) are from a follow-up test session using each participant's user-dependent minimum metabolic cost parameter set  $(k-\theta_0)$  at each speed. (b) Optimal exo stiffness, k, (Nm/rad) and C. equilibrium angle,  $\theta_0$ , (%P2P) for each walking speed (m/s). User-dependent (black) and user-independent (dark gray) follow same convention as A. Statistically significant differences per speed from ZI are indicated by "#" and difference between conditions per speed are indicated by "\*".

analyses (factor: exo condition: ZI, user-ind., user-dep., validation) (Fig. 3(a)) with pairwise post hoc comparisons using a Bonferroni correction. Hypothesis 2 was tested using a single, two-way ANOVA across speed and exo condition (factors: speed: 1.0, 1.3, 1.6 m/s; exo condition: user-ind., user-dep.) (Fig. 3(b), (c)).

A post-hoc linear regression analysis was performed to examine the relationship between changes in users' muscle activity and metabolic cost due to exo assistance (i.e.,  $\Delta$ 's from ZI). The muscles used in the final linear regression were selected by first conducting regressions for each muscle, one-by-one, in a stepwise fashion. At each step, the muscle that yielded the highest increase in the adjusted r-squared of the overall fit was added to the regression (akin to sequential forward selection), yielding an ordering that produced the highest combined adjusted r-squared fit. This process was repeated until all eight recorded muscles were used in the regression (Fig. 6, top). The combination of four muscles with the highest total adjusted r-squared fit was used for further analysis. We constrained the linear regression to have positive coefficients for each muscle; however, the value of the bias term was unconstrained. The participant-average fit equation, r-square, and p-value were computed using the fitted change in muscle activity vs. change in metabolic cost data at each walking speed (Fig. 6, bottom).

#### III. RESULTS

### A. Metabolic Cost

Gross metabolic rate was significantly reduced with optimal semi-active hip exoskeleton impedance control settings (k- $\theta$ 0) for all walking speeds during sweep sessions, but not in the validation session (Fig. 3). During parameter sweep sessions,

when compared to the zero-impedance (ZI) condition, user-dependent optimal parameters reduced gross metabolic rate from ZI by (mean  $\pm$  standard deviation):  $-9.1 \pm 5.7\%$  (p < 0.001) at 1.0 m/s,  $-12.2 \pm 5.2\%$  (p < 0.001) at 1.3 m/s, and  $-9.7 \pm 3.7\%$  (p < 0.001) at 1.6 m/s. (Fig. 3(a) (black), Supp. Fig. 1) User-independent analysis indicated smaller but still significant metabolic reductions from ZI at all but the fastest walking speed:  $-6.5 \pm 4.7\%$  (p = 0.021) at 1.0 m/s,  $-9.8 \pm 1.3\%$  (p = 0.001) at 1.3 m/s, and  $-5.4 \pm 5.5\%$  (p = 0.098) at 1.6 m/s (Fig. 3(a) (dark gray), Fig. 5, right column).

Direct comparison of optimal hip exoskeleton impedance parameters indicated larger reductions in metabolic rate for the user-dependent versus user-independent settings for the fastest but not the slower speeds: p = 0.054 at 1.0 m/s, p = 0.115 at 1.3 m/s, and p = 0.027 at 1.6 m/s (Fig. 3(a), black versus dark grey).

During the validation test sessions (i.e., a re-test of each user's speed-dependent best exoskeleton parameters from sweeps (see Supp. Fig. 1)), we found no significant reduction in gross metabolic rate from ZI at any walking speed:  $-2.1 \pm 4.2\%$  (p = 1.00) at 1.0 m/s,  $-4.0 \pm 6.7\%$  (p = 0.65) at 1.3 m/s, and 4.5  $\pm$  5.7% (p = 0.24) at 1.6 m/s.

# B. Metabolically Optimal Exoskeleton Impedance Control Parameters

The hip exoskeleton impedance control parameters  $(k-\theta_0)$  that minimized metabolic rate were highly variable across participants and showed no significant differences across walking speed (Fig. 3(b) & (c); Fig. 5, right column; Supp. Fig. 1).

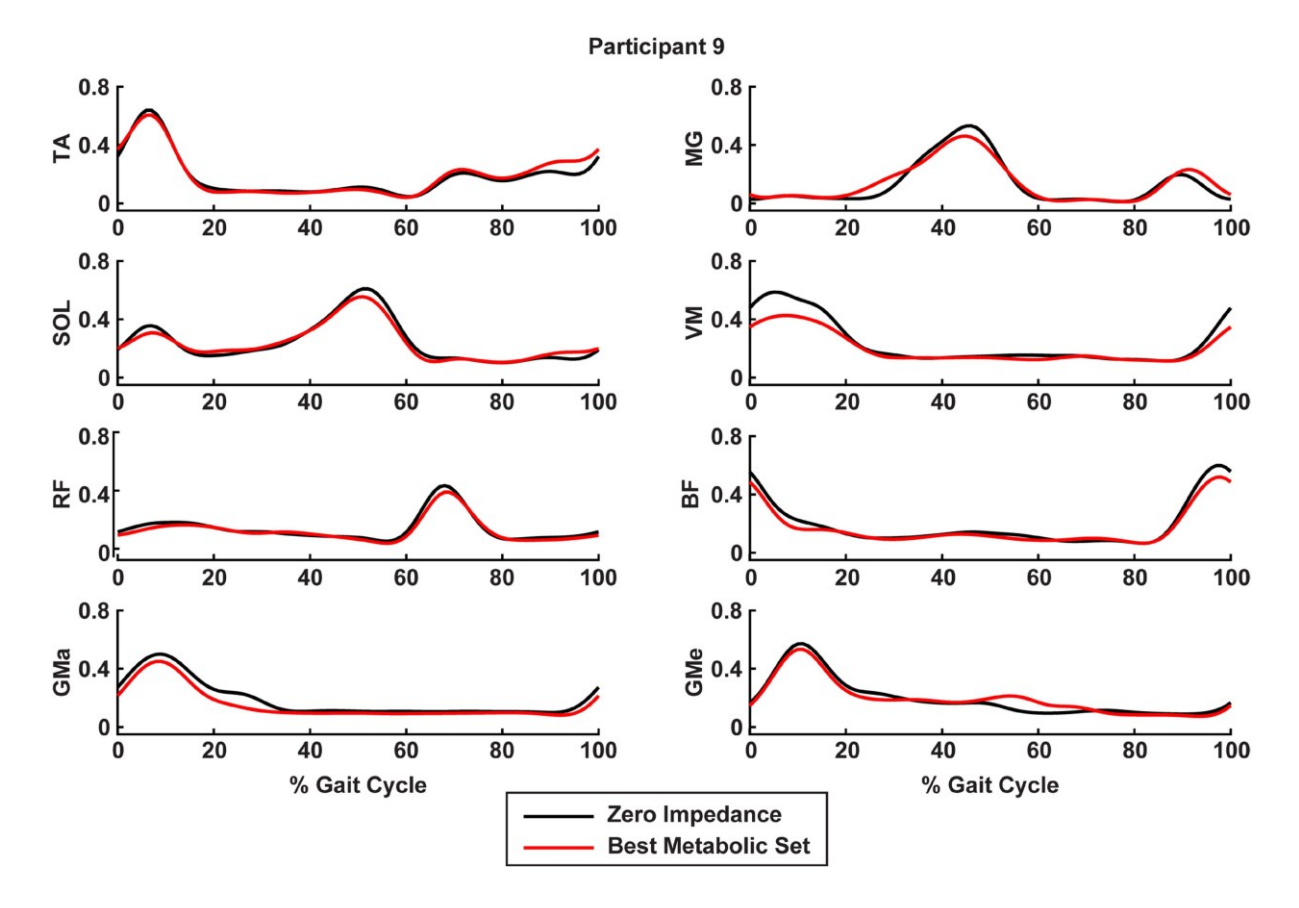


Fig. 4. Muscle activity time-series for the hip exoskeleton impedance parameters ( $k-\theta_0$ ) with the lowest (best) metabolic cost and zero impedance (no assistance or resistance applied to the user). Representative gait cycle (0% heel strike, 60% end stance, to 100% end swing) averaged muscle activity taken from surface electromyography records for Participant 9 during the 1.3 m/s exo parameter sweep session. Black curves are from the zero-impedance condition and red curves are from the condition with exo parameters that were metabolically optimal (k=120 Nm/rad and  $\theta_0=13\%$  P2P). Muscle activity was recorded from 8 lower limb muscles (ordered from distal-to-proximal, anterior-to-posterior): tibialis anterior (TA), medial gastrocnemius (MG), soleus (SOL), vastus medialis (VM), rectus femoris (RF), biceps femoris (BF), gluteus maximus (GMa), and gluteus medius (GMe). The optimal assistance strategy showed reduced hip and knee extensor (e.g., GMa, BF, and VM) activity in early stance and reduced hip flexor activity in early swing (e.g., RF) as well as reduced plantarflexor activity at push-off (e.g., SOL and MG).

Optimal stiffness (*k*) ranged between 40–80 Nm/rad (User-dependent (mean  $\pm$  standard deviation): 44.60  $\pm$  23.01 Nm/rad at 1.0 m/s; 61.75  $\pm$  36.45 Nm/rad at 1.3 m/s and 73.20  $\pm$  35.45 Nm/rad at 1.6 m/s) and increased with walking speed, albeit insignificantly (ANOVA: p = 0.101) (Fig. 3(b), black; Fig. 5, right column). Optimal equilibrium angle ( $\theta_0$ ) was relatively constant around 20% of the peak-to-peak hip angle range of motion (User-dependent: 22.4  $\pm$  13.9 at 1.0 m/s; 20.4  $\pm$  7.6 at 1.3 m/s and 18.1  $\pm$  9.43 at 1.6 m/s) and tended to decrease (i.e., became more extension biased) with increasing walking speed (ANOVA: p = 0.707) (Fig. 3(c), black; Fig. 5, right column).

The significant amount of variability between participants for both optimal stiffness (k) (Fig. 3(b), Supp. Fig. 1) and equilibrium angle ( $\theta_0$ ) (Fig. 3(c), Supp. Fig. 1) was reflected in differences between user-dependent and user-independent optimal values, especially for stiffness (k) at low walking speeds (Fig. 3. black vs. dark grey bars).

## C. Muscle Activity

Muscle activity was reduced for a subset of muscles, local to the assisted joint, by metabolically optimal semi-active hip exoskeleton impedance control settings (k- $\theta$ 0) for all walking speeds (Figs. 5, 6, bottom). Representative time-series data show that reductions in muscle activity were driven by the hip and knee extensors (GMa, BF, and VM, respectively) early in the gait cycle, the hip flexors in early swing (RF) and the ankle plantarflexors (MG, SOL) at push-off. (Fig. 4).

Stepwise, iterative regression analysis revealed that only the four most significant muscles were necessary to characterize the relationship between changes in metabolic cost and changes in muscle activity, as the adjusted r-squared value did not meaningfully increase when more than four muscles were included in the model (Fig. 6, top).

The muscles that most influenced predicted changes in metabolic rate from changes in muscle activity due to hip exoskeleton assistance depended on walking speed. Iterative linear regression indicated: GMa, BF, VM, GMe at 1.0 m/s; BF, VM, RF, and GMe at 1.3 m/s; and BF, GMa, VM, and SOL at 1.6 m/s (Fig. 6, top). BF and VM were present at all speeds; GMa and GMe present at 2 speeds each.

Participant average fits of the 4 'best'-muscle linear regression models indicated a significant relationship (p < 0.0001) between changes in muscle activity and changes in gross metabolic rate

due to hip exoskeleton impedance control when compared to zero-impedance (ZI) for all walking speeds (Fig. 6, bottom). Correlations were strong at all speeds with r-squared values of 0.65, 0.88 and 0.70 at 1.0, 1.3 and 1.6 m/s, respectively.

#### D. Data Archive

The study data set can be found at: https://sites.gatech.edu/hpl/archival-data-from-publications/.

## IV. DISCUSSION

We used a lab-based emulator to evaluate a semi-active hip exoskeleton concept (i.e., motor, spring, clutch system) (Fig. 1) and measured the physiological response of human users to examine whether: (i) optimal impedance settings (spring stiffness, k and equilibrium angle,  $\theta_0$ ) could reduce metabolic cost across a range of walking speeds (1.0–1.6 m/s), and (ii) whether impedance settings (k,  $\theta_0$ ) for metabolically optimal performance depended on walking speed (Fig. 3).

First, we hypothesized that walking with a hip exoskeleton using metabolically optimal impedance settings  $(k, \theta_0)$  would provide metabolic benefit compared to zero-impedance (ZI) mode at each speed. Indeed, the user-dependent parameter set with the lowest metabolic cost provided significant benefit that ranged from 9-12% depending on walking speed (Fig. 3(a), Supp. Fig. 1). Second, we hypothesized that the metabolically optimal impedance parameters  $(k, \theta_0)$  would change across walking speed, mirroring physiological increases in hip joint quasi-stiffness and peak extension moment with speed [15]. Trends in our data supported this idea, as the optimal stiffness (k) increased from  $\sim$ 40 N-m/rad to  $\sim$ 80 N-m/rad (Fig. 3(b)) and the optimal equilibrium angle  $\theta_0$  decreased from >20% to <20% of the P2P hip angle (i.e., larger extensor torque bias) (Fig. 3(c)) as speed increased from 1.0 to 1.6 m/s.

Optimal hip exoskeleton impedance parameters  $(k, \theta_0)$  followed observed trends in biological moments and quasi-stiffness observed in humans walking at faster and faster speeds. Physiological hip moments increase in both extension and flexion with increasing walking speed [10], [52]. This increase in peakto-peak moment is accompanied by an increase in the flexion quasi-stiffness of the joint, or the ratio change in hip joint moment to change in hip joint angle during early swing [7]. Our metabolically optimal hip exo stiffness (k) also increased with speed, causing higher peak flexion and extension hip exo assistance torques. Similar trends have been reported for passive elastic ankle exoskeletons, where the metabolically optimal stiffness also follows physiological changes in ankle joint quasistiffness with increasing walking speed [9], [20]. More broadly, these results suggest that semi-active exoskeletons design that rely on spring-like elements might be nominally set to match trends in the physiological quasi-stiffness of the target joint across locomotion modes (e.g., surface incline, or roughness). Conversely, human-in-the-loop optimizations of powered (not semi-active) exoskeletons to maximize metabolic cost savings while walking has shown that non-physiological torque profiles are optimal for each lower-limb joint [5], [9], [45], [53]. Perhaps semi-active devices, with both powered and passive elements,

should take inspiration from both physiological and optimized torque/impedance information to provide the most benefit to users.

Notably, speed dependent shifts in optimal hip exoskeleton impedance parameters (for k or  $\theta_0$ ) did not reach statistical significance. This was mostly because of high variability in optimal impedance settings between participants (Fig. 3(b), (c); Supp. Fig. 1), and highlights the potential importance of focusing on tuning exo control parameters to each individual user to maximize performance (i.e., user-dependent controller settings). Indeed, differences between hip exo impedance parameter (k,  $\theta_0$ ) - metabolic cost landscapes derived using a user-dependent (i.e., per-each individual, or customized) (Supp. Fig. 1) versus a user-independent (i.e., averaged across-individuals or generalized) (Fig. 5) analysis approach points to the potential benefit of tuning assistance to each unique user (i.e., personalized control). For example, for the metabolically optimal stiffness (k), the user-dependent values increased steadily with walking speed while the user-independent values only appeared to increase at 1.6 m/s (Fig. 3(b)). This suggests that the effect of increased stiffness (k), (i.e., higher hip exo torque for both flexion and extension) did not yield a large generalized metabolic benefit for most users across speed, but instead, a subset of users benefited greatly from increased stiffness (k), when moving from 1.0 to 1.3 m/s (Supp. Fig. 1, Participants 4, 7, 8, 9). Thus, using a semi-active device hip exo with stiffness tuned for the average user (i.e., user-independent) at intermediate speed would leave some users with a glaring lack of metabolic benefit. Indeed, user-dependent assistance tended to provide more metabolic benefit than user-independent stiffness at every walking speed (Fig. 3(a)). Other studies comparing user-dependent (customized) vs. user-independent (generalized) torque profiles with powered ankle exoskeletons also show increased benefits from a user-dependent approach - both for increasing preferred walking speed [54] and reducing metabolic cost [5], [45] compared to a user-independent 'one-size-fits all' approach. Taken together, these data suggest that perhaps commercial exoskeletons could apply a generalized 'best' assistance profile for 'out-of-the-box use' but that control settings should then be customized per user to provide highest possible benefit.

Muscles ultimately consume the metabolic energy that moves us, and exoskeletons reduce metabolic cost principally by reducing muscle force and activation [55]–[57]. Our data strongly support this idea, as changes in activity of the lower-limb muscles had strong correlation with changes in metabolic cost due to torque assistance from our semi-active hip exoskeleton concept (Figs. 5, 6). The strength of the fits from our linear regression analyses at all walking speeds (Fig. 6, bottom) supports the validity of using a multi-channel surface electromyography (EMG) approach to model metabolic cost of exoskeleton users rather than direct measurements via indirect calorimetry [58], [59]. Using changes in EMG as a proxy for changes in metabolic cost could allow for faster on-line tuning of exoskeletons control parameters than what is offered by traditional human-in-the loop approaches.

Changes in activity of the muscles spanning the hip joint (e.g., GMa, GMe, BF, RF) were shown to be most significant

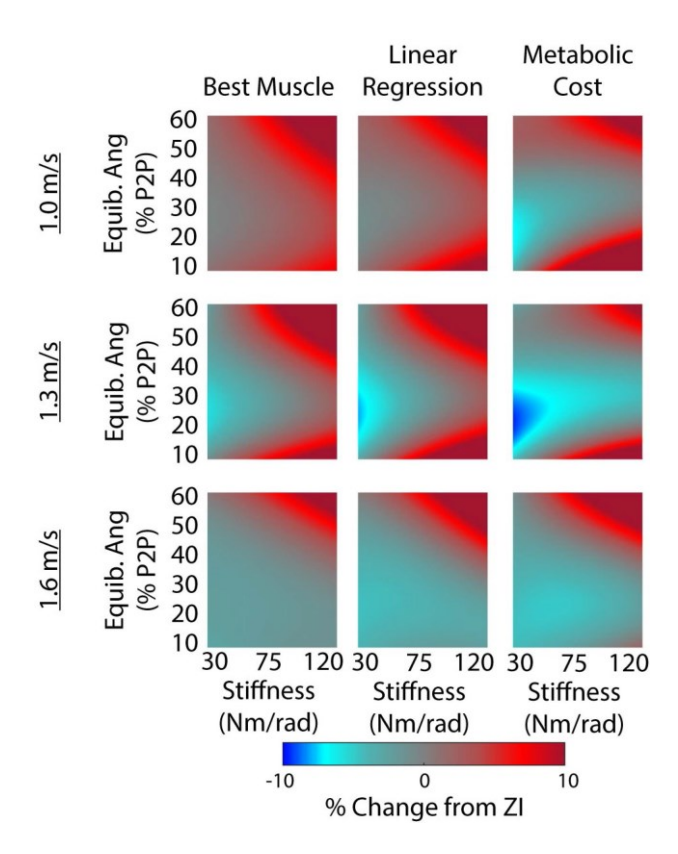


Fig. 5. User-independent changes in muscle activity and metabolic cost across hip exoskeleton impedance parameter space (k- $\theta_0$ ): Acrossparticipant averaged (i.e., user-independent) multidimensional polynomial fits to sampled percentage change (red = increase; blue = decrease from the zero-impedance (ZI) condition) for each exoskeleton impedance parameter setting (a 5x6 stiffness (k) vs. equilibrium angle  $(\theta_0)$  grid space) at each walking speed (1.0 m/s (top row), 1.3 m/s, 1.6 m/s (bottom row)). Columns represent different outcome measures. (Left) Total muscle activity from the muscle with the best linear regression fit to metabolic cost (Best Muscle), (Middle) Linear regression fit using the 4 muscles with the best combined fit to metabolic cost (Linear Regression), and (Right) metabolic cost. The muscles selected per speed for the Best Muscle and Linear Regression fits can be found in Fig. 5 top row. The method of selecting muscles for the linear regressions is discussed in Section II-E. In general, a semi-active hip impedance controller with low stiffness and equilibrium angle working at an intermediate walking speed had the most benefit. Study-wide, changes in muscle activity corresponded well with changes in metabolic

in predicting changes in metabolic cost (Fig. 5, top); perhaps not surprising given the primary action of the exo is about the hip. Indeed, many other studies have shown that when robotic exoskeletons target the knee or ankle joint, the muscles that are more closely associated with those joints tend to respond most and drive changes in users' metabolic cost [8], [60], [61]. However, it is interesting to note that hip assistance also helped reduce activity in the knee extensors (VM) during early stance and the plantarflexors (SOL, MG) in late stance (Fig. 4), re-emphasizing results from previous studies showing that exos at the hip [62] and ankle [63] can have non-local effects on muscle effort.

Metabolic benefit shown for optimal semi-active hip exoskeleton parameters  $(k, \theta_0)$  of the metabolic cost landscape across parameters from the comprehensive sweep sessions did

not transfer to the validation session for any walking speed (Fig. 3(a)). We believe the lack of translation was due to the limited time given for re-habituation to optimal exoskeleton assistance from the sweep sessions at each walking speed. Habituation to exoskeleton assistance can occur in as little as 20 minutes [8], [44], [64], [65] but on average probably takes much longer, especially for metabolic rate to reach a new-steady state [45]. Much less is known about how habituation persists across multiple use-sessions separated by a significant time (i.e., retention form one session to another) and/or how long is needed to re-habituate. Our results provide some evidence that re-habituation may be crucial. One could posit that our results from the sweep session were biased by measurement noise inherent when using indirect calorimetry to measure metabolic rate and further exacerbated by 2-minute estimations of steady-state cost, rather than effects of the exoskeleton control parameters themselves. To avoid this problem, we fit a multi-polynomial surface to the change in metabolic rate versus zero-impedance (ZI) across the grid of exoskeleton impedance parameters (k,  $\theta_0$ ), and then selected the optimal parameters based on the estimated metabolic minimum of the fit. Thus, the optimal set  $(k, \theta_0)$ , was influenced by all data points in the measurement set that generated fitted surface, decreasing bias from outliers and/or measurement noise (assumed to be normally-distributed). Further, the difference in metabolic rate from ZI for our optimal parameter sets is much larger than the noise associated with measures of metabolic rate from indirect calorimetry [50], [66]. Strong correlations between changes in metabolic cost and changes in muscle activity ( $R^2 = 0.52-0.78$ ) provide some physiological evidence that our measured changes were due to the exoskeleton and not measurement noise or bias.

Our study was not without some limitations. First, our hip exoskeleton end effector hardware was designed to handle over 200 Nm of torque applied at the hip [41]. Considering this, the added mass of the exoskeleton was much larger than what would be expected for a portable, autonomous semi-active version of the device. To accommodate for this difference, we compared gross metabolic rate in active impedance trials to that of wearing the exoskeleton in zero-impedance (ZI) mode, but we note that the bulk of the emulator may have affected the measured metabolically optimal assistance parameters  $(k, \theta_0)$ themselves. Second, our emulator did not perfectly reproduce the semi-active device due to safety adjustments made to the onset of extension torque and imperfect torque tracking. As mentioned in Section II-A, we implemented a ramp function to decrease the speed of extension torque onset from ZI mode as some pilot users found this uncomfortable. The consequence of this ramp was decreased peak extension torques. Root-meansquared-error of torque tracking across conditions was ~3 Nm, which equated to <15% of peak-to-peak torque. We believed this was reasonable to conduct the study as torques generally followed the desired passive spring torque, but we acknowledge this does not perfectly emulate the proposed semi-active device. Last, this study was conducted on a treadmill rather than overground, which could have limited user adaptation via free adjustments in walking speed. Exoskeleton assistance has been shown to alter preferred walking speed along with changes in

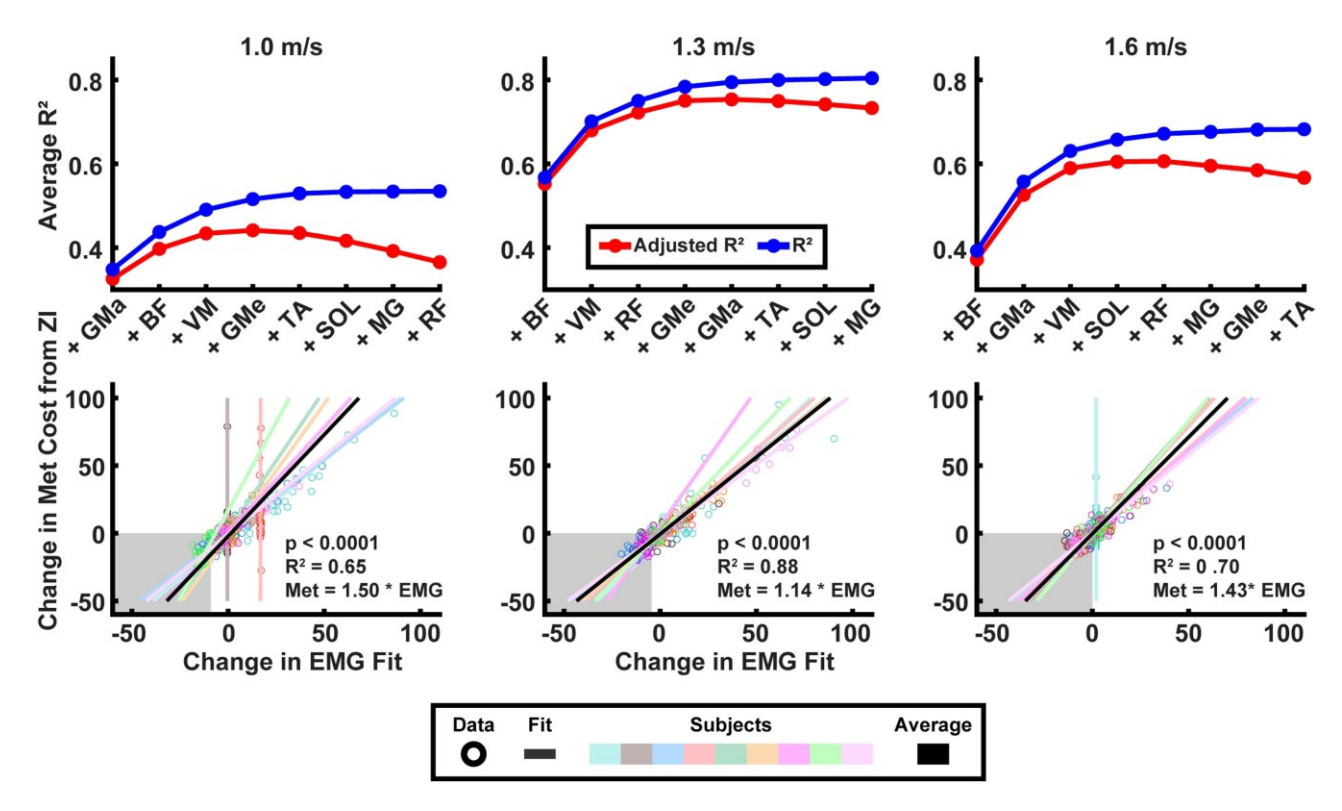


Fig. 6. Association between changes in users' lower-limb muscle activity and metabolic cost across hip exoskeleton impedance parameter space  $(k-\theta_0)$ : (Top) Participant average r-squared and adjusted r-squared values produced in an iterative regression process, relating changes in gait cycle averaged muscle activity (%) and changes in gross metabolic rate (%) compared to the zero-impedance (ZI) condition. On the x-axis, the muscles included in the model are cumulative from left to right, so that each muscle's plotted r-squared point corresponds with a model that also includes all muscles in the preceding columns. Data are separated by walking speed (1.0 m/s, 1.3 m/s, 1.6 m/s form left to right). (Bottom) Linear regression fits using the four most significant muscles (i.e., four 'best' fits) per participant (colored lines) and the averaged across participants (black lines) for walking at 1.0 m/s, 1.3 m/s, and 1.6 m/s (left to right). Grey boxes highlight the areas in which there was a reduction in metabolic rate with respect to the corresponding zero-impedance (ZI) trial. Study-wide, changes in muscle activity corresponded well with changes in metabolic rate and participants who derived metabolic benefit had reduced muscle activity, especially at faster walking speeds.

metabolic cost [24], [54]. Thus, it is possible that metabolic benefits could be higher for walking speeds outside the range we tested. future studies could explore optimizing the global cost of transport (i.e., energy consumption per distance travelled), where both metabolic rate and preferred walking speed can equally contribute. This scenario might better represent user behavior outside of the lab, as humans tend to select their preferred walking speed to minimize cost of transport [67] in real-time [68], [69]. In our future work, rather than using an in the lab emulator to perform brute force exoskeleton controller parameter sweeps during treadmill walking at fixed speed, we plan to conduct optimizations using autonomous devices outside the lab under real-world conditions that better represent an average user's daily activities.

# V. CONCLUSION

A tethered hip exoskeleton emulating semi-active hardware, via spring-like impedance control, can reduce metabolic cost by up to  $\sim 10\%$  compared to zero-impedance (ZI) across functional walking speeds (1.3–1.6 m/s). Stiffer springs, with an equilibrium angle set to provide higher magnitude hip extension assistance throughout more of the gait cycle, tended to perform better at faster walking speeds. Tuning impedance control

parameters to each individual user and longer training periods are likely to further improve performance. Local muscle activity (e.g., glutes, hamstrings) could be an important physiological input as a proxy for metabolic demand for online optimization of controller parameters to continuously minimize metabolic cost during unstructured, 'real-world' locomotion. This paves the way and provides crucial guidance for developing energy efficient, portable semi-active assistance strategies at the hip across walking speed.

## **ACKNOWLEDGMENT**

The authors would like to acknowledge Matias Teixeira-Prates, Jiun-Jie Yang, Andrew Lockhart, Sasikumaran Nandakumar, Reagan Cook, Eric Salisbury for their assistance during pilot testing and data collection, and members of the Stanford Biomechatronics Lab (Gwen Bryan, Patrick Franks, and Stefan Klein) for assistance with fabrication, calibration, and pilot testing of the hip exoskeleton end effector hardware.

## **REFERENCES**

[1] G. S. Sawicki et al., "The exoskeleton expansion: Improving walking and running economy," *J. Neuroeng. Rehabil.*, vol. 17, no. 1, pp. 17–25, Feb. 2020, doi: 10.1186/s12984-020-00663-9.

- [2] S. Galle et al., "Reducing the metabolic cost of walking with an ankle exoskeleton: Interaction between actuation timing and power," *J. Neu-roeng. Rehabil.*, vol. 14, no. 1, pp. 14–35, Apr. 2017, doi: 10.1186/s12984-017-0235-0.
- [3] K. Seo, J. Lee, and Y. J. Park, "Autonomous hip exoskeleton saves metabolic cost of walking uphill," in *Proc. IEEE Int. Conf. Rehabil. Robot.*, 2017, vol. 2017, pp. 246–251, doi: 10.1109/ICORR.2017.8009254.
- [4] A. J. Young et al., "Influence of power delivery timing on the energetics and biomechanics of humans wearing a hip exoskeleton," Frontiers Bioeng. Biotechnol., vol. 5, 2017, Art. no. 4, doi: 10.3389/fbioe.2017.00004.
- [5] J. Zhang et al., "Human-in-the-loop optimization of exoskeleton assistance during walking," *Science*, vol. 356, no. 6344, pp. 1280–1284, Jun. 2017, doi: 10.1126/science.aal5054.
- [6] J. Kim et al., "Reducing the metabolic rate of walking and running with a versatile, portable exosuit," *Science*, vol. 365, no. 6454, pp. 668–672, Aug. 2019, doi: 10.1126/science.aav7536.
- [7] G. Lee et al., "Reducing the metabolic cost of running with a tethered soft exosuit," *Sci. Robot.*, vol. 2, no. 6, May 2017, Art. no. eaan6708, doi: 10.1126/scirobotics.aan6708.
- [8] R. W. Nuckols and G. S. Sawicki, "Impact of elastic ankle exoskeleton stiffness on neuromechanics and energetics of human walking across multiple speeds," *J. Neuroeng. Rehabil.*, vol. 17, no. 1, Jun. 2020, Art. no. 5, doi: 10.1186/s12984-020-00703-4.
- [9] G. M. Bryan et al., "Optimized hip-knee-ankle exoskeleton assistance at a range of walking speeds," *J. Neuroeng. Rehabil.*, vol. 18, no. 1, Oct. 2021, Art. no. 152, doi: 10.1186/s12984-021-00943-y.
- [10] D. J. Farris and G. S. Sawicki, "The mechanics and energetics of human walking and running: A joint level perspective," *J. Roy. Soc. Interface*, vol. 9, no. 66, pp. 110–118, Jan. 2012, doi: 10.1098/rsif.2011.0182.
- [11] R. W. Nuckols et al., "Mechanics of walking and running up and downhill: A joint-level perspective to guide design of lower-limb exoskeletons," *PLoS One*, vol. 15, no. 8, 2020, Art. no. e0231996, doi: 10.1371/jour-nal.pone.0231996.
- [12] R. Ř. Neptune, K. Sasaki, and S. A. Kautz, "The effect of walking speed on muscle function and mechanical energetics," *Gait Posture*, vol. 28, no. 1, pp. 135–143, Jul. 2008, doi: 10.1016/j.gaitpost.2007.11.004.
- [13] J. M. Donelan, R. Kram, and A. D. Kuo, "Mechanical work for step-to-step transitions is a major determinant of the metabolic cost of human walking," J. Exp. Biol., vol. 205, no. 23, pp. 3717–3727, Dec. 2002. [Online]. Available: https://www.ncbi.nlm.nih.gov/pubmed/12409498
- [14] K. E. Zelik, K. Z. Takahashi, and G. S. Sawicki, "Six degree-of-freedom analysis of hip, knee, ankle and foot provides updated understanding of biomechanical work during human walking," *J. Exp. Biol.*, vol. 218, no. 6, pp. 876–886, Mar. 2015, doi: 10.1242/jeb.115451.
- [15] K. Shamaei, G. S. Sawicki, and A. M. Dollar, "Estimation of quasi-stiffness of the human hip in the stance phase of walking," *PLoS One*, vol. 8, no. 12, 2013, Art. no. e81841, doi: 10.1371/journal.pone.0081841.
- [16] K. Shamaei, G. S. Sawicki, and A. M. Dollar, "Estimation of quasi-stiffness and propulsive work of the human ankle in the stance phase of walking," *PLoS One*, vol. 8, no. 3, 2013, Art. no. e59935, doi: 10.1371/journal.pone.0059935.
- [17] K. Shamaei, G. S. Sawicki, and A. M. Dollar, "Estimation of quasi-stiffness of the human knee in the stance phase of walking," *PLoS One*, vol. 8, no. 3, 2013, Art. no. e59993, doi: 10.1371/journal.pone.0059993.
- [18] D. J. Farris and B. J. Raiteri, "Modulation of leg joint function to produce emulated acceleration during walking and running in humans," *Roy. Soc. Open Sci.*, vol. 4, no. 3, Mar. 2017, Art. no. 160901, doi:10.1098/rsos.160901.
- [19] D. J. Farris and B. J. Raiteri, "Elastic ankle muscle-tendon interactions are adjusted to produce acceleration during walking in humans," *J. Exp. Biol.*, vol. 220, no. 22, pp. 4252–4260, Nov. 2017, doi: 10.1242/jeb.159749.
- [20] B. R. Umberger and J. Rubenson, "Understanding muscle energetics in locomotion: New modeling and experimental approaches," *Exercise Sport Sci. Rev.*, vol. 39, no. 2, pp. 59–67, Apr. 2011, doi: 10.1097/ JES.0b013e31820d7bc5.
- [21] G. S. Sawicki, C. L. Lewis, and D. P. Ferris, "It pays to have a spring in your step," *Exercise Sport Sci. Rev.*, vol. 37, no. 3, pp. 130–138, Jul. 2009, doi: 10.1097/JES.0b013e31819c2df6.
- [22] R. C. Browning et al., "The effects of adding mass to the legs on the energetics and biomechanics of walking," *Med. Sci. Sports Exercise*, vol. 39, no. 3, pp. 515–525, Mar. 2007, doi: 10.1249/mss.0b013e 31802b3562.
- [23] F. A. Panizzolo et al., "Effect of a passive hip exoskeleton on walking distance in neurological patients," Assist. Technol., pp. 1–6, Mar. 2021, doi: 10.1080/10400435.2021.1880494.

- [24] F. A. Panizzolo et al., "Reducing the energy cost of walking in older adults using a passive hip flexion device," *J. Neuroeng. Rehabil.*, vol. 16, no. 1, Oct. 2019, Art. no. 160901, doi: 10.1186/s12984-019-0599-4.
- [25] F. A. Panizzolo et al., "Metabolic cost adaptations during training with a soft exosuit assisting the hip joint," *Sci. Rep.*, vol. 9, no. 1, Jul. 2019, Art. no. 9779, doi: 10.1038/s41598-019-45914-5.
- [26] K. Shamaei et al., "Preliminary investigation of effects of a quasi-passive knee exoskeleton on gait energetics," in *Proc. 36th Annu. Int. Conf. IEEE Eng. Med. Biol. Soc.*, 2014, pp. 3061–3064.
- [27] K. Shamaei et al., "Design and evaluation of a quasi-passive knee exoskeleton for investigation of motor adaptation in lower extremity joints," *IEEE Trans. Biomed. Eng.*, vol. 61, no. 6, pp. 1809–1821, Jun. 2014, doi: 10.1109/TBME.2014.2307698.
- [28] A. J. Young, H. Gannon, and D. P. Ferris, "A biomechanical comparison of proportional electromyography control to biological torque control using a powered hip exoskeleton," *Front. Bioeng. Biotechnol.*, vol. 5, 2017, Art. no. 37, doi: 10.3389/fbioe.2017.00037.
- [29] J. Lee et al., "Effects of assistance timing on metabolic cost, assistance power, and gait parameters for a hip-type exoskeleton," in *Proc. Int. Conf. Rehabil. Robot.*, 2017, pp. 498–504. [Online]. Available: <Go to ISI>: //WOS:000426850800086
- [30] B. Lim et al., "Delayed output feedback control for gait assistance with a robotic hip exoskeleton," *IEEE Trans. Robot.*, vol. 35, no. 4, pp. 1055–1062, Aug. 2019, doi: 10.1109/Tro.2019.2913318.
- [31] M. K. Shepherd and E. J. Rouse, "The VSPA foot: A quasi-passive ankle-foot prosthesis with continuously variable stiffness," *IEEE Trans. Neural Syst. Rehabil. Eng.*, vol. 25, no. 12, pp. 2375–2386, Dec. 2017, doi: 10.1109/TNSRE.2017.2750113.
- [32] E. M. Glanzer and P. G. Adamczyk, "Design and validation of a semiactive variable stiffness foot prosthesis," *IEEE Trans. Neural Syst. Rehabil. Eng.*, vol. 26, no. 12, pp. 2351–2359, Dec. 2018, doi: 10.1109/ TNSRE.2018.2877962.
- [33] J. K. Leestma, K. H. Fehr, and P. G. Adamczyk, "Adapting semiactive prostheses to real-world movements: Sensing and controlling the dynamic mean ankle moment arm with a variable-stiffness foot on ramps and stairs," *Sensors (Basel)*, vol. 21, no. 18, Sep. 2021, Art. no. 6009, doi: 10.3390/s21186009.
- [34] H. L. Bartlett et al., "A semipowered ankle prosthesis and unified controller for level and sloped walking," *IEEE Trans. Neural Syst. Rehabil. Eng.*, vol. 29, pp. 320–329, 2021, doi: 10.1109/Tnsre.2021.3049194.
- [35] D. J. Braun et al., "Variable stiffness spring actuators for low-energy-cost human augmentation," *IEEE Trans. Robot.*, vol. 35, no. 6, pp. 1435–1449, Dec. 2019, doi: 10.1109/Tro.2019.2929686.
- [36] D. J. Braun, V. Chalvet, and A. Dahiya, "Positive-Negative stiffness actuators," *IEEE Trans. Robot.*, vol. 35, no. 1, pp. 162–173, Feb. 2019, doi: 10.1109/Tro.2018.2872284.
- [37] V. Chalvet and D. J. Braun, "Algorithmic design of low-power variablestiffness mechanisms," *IEEE Trans. Robot.*, vol. 33, no. 6, pp. 1508–1515, Dec. 2017, doi: 10.1109/Tro.2017.2719049.
- [38] V. Chalvet and D. J. Braun, "Criterion for the design of low-power variable stiffness mechanisms," *IEEE Trans. Robot.*, vol. 33, no. 4, pp. 1002–1010, Aug. 2017, (in English), doi: 10.1109/Tro.2017.2689068.
- [39] A. Sutrisno and D. J. Braun, "Enhancing mobility with quasipassive variable stiffness exoskeletons," *IEEE Trans. Neural Syst. Rehabil. Eng.*, vol. 27, no. 3, pp. 487–496, Mar. 2019, doi: 10.1109/ TNSRE.2019.2899753.
- [40] C. G. Welker et al., "Shortcomings of human-in-the-loop optimization of an ankle-foot prosthesis emulator: A case series," *Roy. Soc. Open Sci.*, vol. 8, no. 5, May 2021, Art. no. 202020, doi: 10.1098/rsos.202020.
- [41] G. M. Bryan et al., "A hip-knee-ankle exoskeleton emulator for studying gait assistance," *Int. J. Robot. Res.*, vol. 40, no. 4-5, pp. 722–746, 2020, doi: 10.1177/0278364920961452.
- [42] B. Whittington et al., "The contribution of passive-elastic mechanisms to lower extremity joint kinetics during human walking," *Gait Posture*, vol. 27, no. 4, pp. 628–634, May 2008, doi: 10.1016/j.gaitpost.2007.08.005.
- [43] P. W. Franks et al., "Comparing optimized exoskeleton assistance of the hip, knee, and ankle in single and multi-joint configurations," *Wearable Technol.*, vol. 2, 2021, Art. no. e16, doi: 10.1017/wtc.2021.14.
- [44] S. Galle et al., "Adaptation to walking with an exoskeleton that assists ankle extension," *Gait Posture*, vol. 38, no. 3, pp. 495–499, Jul. 2013, doi: 10.1016/j.gaitpost.2013.01.029.
- [45] K. L. Poggensee and S. H. Collins, "How adaptation, training, and customization contribute to benefits from exoskeleton assistance," *Sci. Robot.*, vol. 6, no. 58, Sep. 2021, Art. no. eabf1078, doi: 10.1126/ scirobotics.abf1078.

- [46] W. Felt et al., "'Body-in-the-loop': Optimizing device parameters using measures of instantaneous energetic cost," *PLoS One*, vol. 10, no. 8, 2015, Art. no. e0135342, doi: 10.1371/journal.pone.0135342.
- [47] J. Zhang et al., "Human-in-the-loop optimization of exoskeleton assistance during walking," *Science*, vol. 356, pp. 1280–1283, 2017, doi: 10.1126/science.aal5054.
- [48] M. Kim et al., "Human-in-the-loop Bayesian optimization of wearable device parameters," *PLoS ONE*, vol. 12, no. 9, pp. 6–8, 2017, doi: 10.1371/journal.pone.0184054.
- [49] J. M. Brockway, "Derivation of formulas used to calculate energy-expenditure in man," *Human Nutr. Clin. Nutr.*, vol. 41, no. 6, pp. 463–471, Nov. 1987. [Online]. Available: <GotoISI>://WOS:A1987L345600006
- [50] J. C. Selinger and J. M. Donelan, "Estimating instantaneous energetic cost during non-steady-state gait," *J. Appl. Physiol.*, vol. 117, no. 11, pp. 1406–1415, Dec. 2014, doi: 10.1152/japplphysiol.00445.2014.
- [51] P. Konrad, ABC of EMG A Practical Introduction to Kinesiological Electromyography. Scottsdale, AZ, USA: Noraxon USA, 2005.
- [52] J. Camargo et al., "A comprehensive, open-source dataset of lower limb biomechanics in multiple conditions of stairs, ramps, and level-ground ambulation and transitions," *J. Biomech.*, vol. 119, Apr. 2021, Art. no. 110320, doi: 10.1016/j.jbiomech.2021.110320.
- [53] G. M. Bryan et al., "Optimized hip-knee-ankle exoskeleton assistance reduces the metabolic cost of walking with worn loads," J. Neuroeng. Rehabil., vol. 18, no. 1, Nov. 2021, Art. no. 161, doi: 10.1186/s12984-021-00955-8.
- [54] S. Song and S. H. Collins, "Optimizing exoskeleton assistance for faster self-selected walking," *IEEE Trans. Neural Syst. Rehabil. Eng.*, vol. 29, pp. 786–795, 2021, doi: 10.1109/TNSRE.2021.3074154.
- [55] O. N. Beck et al., "Exoskeletons improve locomotion economy by reducing active muscle volume," *Exercise Sport Sci. Rev.*, vol. 47, no. 4, pp. 237–245, Oct. 2019, doi: 10.1249/JES.0000000000000204.
- [56] R. W. Nuckols et al., "Ultrasound imaging links soleus muscle neuromechanics and energetics during human walking with elastic ankle exoskeletons," Sci. Rep., vol. 10, no. 1, Feb. 2020, Art. no. 3604, doi: 10.1038/s41598-020-60360-4.
- [57] M. Shepertycky et al., "Removing energy with an exoskeleton reduces the metabolic cost of walking," *Science*, vol. 372, no. 6545, pp. 957–960, May 2021, doi: 10.1126/science.aba9947.
- [58] K. A. Ingraham, D. P. Ferris, and C. D. Remy, "Evaluating physiological signal salience for estimating metabolic energy cost from wearable sensors," *J. Appl. Physiol.*, vol. 126, no. 3, pp. 717–729, Mar. 2019, doi: 10.1152/japplphysiol.00714.2018.

- [59] P. Slade et al., "Rapid energy expenditure estimation for ankle assisted and inclined loaded walking," J. Neuroeng. Rehabil., vol. 16, no. 1, Jun. 2019, Art. no. 67, doi: 10.1186/s12984-019-0535-7.
- [60] B. A. Shafer et al., "Neuromechanics and energetics of walking with an ankle exoskeleton using neuromuscular-model based control: A parameter study," *Frontiers Bioeng. Biotechnol.*, vol. 9, 2021, Art. no. 615358, doi: 10.3389/fbioe.2021.615358.
- [61] D. Lee et al., "Effects of assistance during early stance phase using a robotic knee orthosis on energetics, muscle activity, and joint mechanics during incline and decline walking," *IEEETrans. Neural Syst. Rehabil. Eng.*, vol. 28, no. 4, pp. 914–923, Apr. 2020, doi: 10.1109/TNSRE.2020.2972323.
- [62] T. Lenzi, M. C. Carrozza, and S. K. Agrawal, "Powered hip exoskeletons can reduce the user's hip and ankle muscle activations during walking," *IEEE Trans. Neural Syst. Rehabil. Eng.*, vol. 21, no. 6, pp. 938–948, Nov. 2013, doi: 10.1109/TNSRE.2013.2248749.
- [63] J. R. Koller et al., "Learning to walk with an adaptive gain proportional myoelectric controller for a robotic ankle exoskeleton," *J. Neuroeng. Rehabil.*, vol. 12, Nov. 2015, Art. no. 97, doi: 10.1186/s12984-015-0086-5.
- [64] S. M. Cain, K. E. Gordon, and D. P. Ferris, "Locomotor adaptation to a powered ankle-foot orthosis depends on control method," *J. Neuroeng. Rehabil.*, vol. 4, Dec. 2007, Art. no. 48, doi: 10.1186/1743-0003-4-48.
- [65] K. E. Gordon and D. P. Ferris, "Learning to walk with a robotic ankle exoskeleton," *J. Biomech.*, vol. 40, no. 12, pp. 2636–2644, 2007, doi: 10.1016/j.jbiomech.2006.12.006.
- [66] J. R. Koller et al., "Confidence in the curve: Establishing instantaneous cost mapping techniques using bilateral ankle exoskeletons," *J. Appl. Physiol.*, vol. 122, no. 2, pp. 242–252, Feb. 2017, doi: 10.1152/japplphysiol.00710.2016.
- [67] H. J. Ralston, "Energy-speed relation and optimal speed during level walking," *Internationale Zeitschrift für Angewandte Physiologie Ein*schliesslich Arbeitsphysiologie, vol. 17, no. 4, pp. 277–283, 1958.
- [68] J. C. Selinger et al., "Humans can continuously optimize energetic cost during walking," *Curr. Biol.*, vol. 25, no. 18, pp. 2452–2456, Sep. 2015, doi: 10.1016/j.cub.2015.08.016.
- [69] J. C. Selinger et al., "How humans initiate energy optimization and converge on their optimal gaits," J. Exp. Biol., vol. 222, no. 19, Oct. 2019, Art. no. jeb198234, doi: 10.1242/jeb.198234.